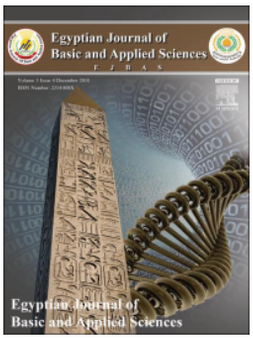

Egyptian Journal of Basic and Applied Sciences

ISSN: (Print) (Online) Journal homepage: www.tandfonline.com/journals/teba20

Unveiling the therapeutic significance of shikimate pathway-derived phenolic acids against penicillin-binding protein 3 of *Pseudomonas aeruginosa*

Yamkela Dweba, Christiana E. Aruwa, Taofeeq Garuba & Saheed Sabiu

To cite this article: Yamkela Dweba, Christiana E. Aruwa, Taofeeq Garuba & Saheed Sabiu (2024) Unveiling the therapeutic significance of shikimate pathway-derived phenolic acids against penicillin-binding protein 3 of *Pseudomonas aeruginosa*, Egyptian Journal of Basic and Applied Sciences, 11:1, 685-706, DOI: 10.1080/2314808X.2024.2401741

To link to this article: https://doi.org/10.1080/2314808X.2024.2401741

EGYPTIAN JOURNAL OF BASIC AND APPLIED SCIENCES
2024, VOL. 11, NO. 1, 685–706
https://doi.org/10.1080/2314808X.2024.2401741

Unveiling the therapeutic significance of shikimate pathway-derived phenolic acids against penicillin-binding protein 3 of *Pseudomonas aeruginosa*

Yamkela Dweba[a], Christiana E. Aruwa[a], Taofeeq Garuba[b] and Saheed Sabiu[a]

[a]Department of Biotechnology and Food Science, Faculty of Applied Sciences, Durban University of Technology (DUT), Durban, South Africa; [b]Department of Plant Biology, University of Ilorin, Ilorin, Nigeria

ABSTRACT

This study investigated the modulatory potential of Shikimate pathway-derived phenolic acids against penicillin-binding protein 3 (PBP3) of *Pseudomonas aeruginosa* using computational and *in vitro* methods. The binding and inhibitory capabilities of 22 phenolic acids against the catalytic site of PBP3 were evaluated and revealed ellagic and chlorogenic acids as the top inhibitors, showing superior docking scores of −8.4 kcal/mol each compared to the standard, cefotaxime (−7.5 kcal/mol). Dynamics simulation of their PBP3 complexes indicated chlorogenic acid's efficacy in inhibiting PBP3 (−33.65 kcal/mol) relative to cefotaxime (−30.10 kcal/mol), while interacting with key catalytically relevant residues. The quantum features analysis using DFT/B3LYP suggested chlorogenic acid's superior reactivity and compatibility with the PBP3 active site. *In vitro* evaluation revealed an MIC of 200 mg/ml for chlorogenic acid and 0.8 mg/ml for cefotaxime against *Pseudomonas aeruginosa* ATCC 27,853, while their combination showed a synergistic action mechanism (FIC index of 0.5). These observations were validated in time-kill kinetics (gradual decrease in viable cells over 24 h). The study concludes chlorogenic acid as promising PBP3 inhibitor. Nonetheless, further studies could focus on the structural modification of chlorogenic acid to improve its pharmacokinetic properties and potential as an antibacterial drug candidate *in vivo*.

ARTICLE HISTORY
Received 12 May 2024
Revised 10 August 2024
Accepted 3 September 2024

KEYWORDS
Penicillin-binding protein; shikimate pathway; phenolic acids; molecular docking; dynamics simulation; antimicrobial resistance

Introduction

Morbidity and death rates associated with *Pseudomonas aeruginosa* infection are a global cause for concern, especially in immunocompromised patients [1]. Infections caused by *P. aeruginosa* have become difficult to treat due to their multi-drug resistance (MDR) to available antibiotics like aminoglycosides, quinolones, carbapenems, β-lactams and cephalosporins like cefepime regarded as the antibiotic of choice in pseudomonal infections therapy [2,3]. As such, this pathogen is one of the bacterial strains contributing tremendously to the ongoing antimicrobial resistance (AMR) crisis. This led to the World Health Organization (WHO) designating *P. aeruginosa* as an important pathogenic species requiring new antimicrobial development to enhance the treatment of associated infections [4]. The extensive use of antibiotics exacerbates drug resistance development in *P. aeruginosa*

CONTACT Saheed Sabiu sabius@dut.ac.za Department of Biotechnology and Food Science, Faculty of Applied Sciences, Durban University of Technology (DUT), PO Box 1334, Durban, KwaZulu-Natal 4000, South Africa

This article has been corrected with minor changes. These changes do not impact the academic content of the article.

Supplemental data for this article can be accessed online at https://doi.org/10.1080/2314808X.2024.2401741

and leads to the ineffectiveness of conventional antibiotics, thus limiting treatment options [5]. This emphasizes the need for and importance of identifying and developing novel antimicrobial agents to combat infections caused by drug-resistant *P. aeruginosa*.

Bacteria rely on the integrity of their cell walls containing peptidoglycan layers for survival, and this layer aids in AMR expression [6,7]. Peptidoglycan comprises a disaccharide with peptide links known as NAG-NAM (N-acetyl glucosamine-N-acetylmuramic acid), on the NAM unit [8]. The synthesis of NAG-NAM subunits and cross-linking of the peptide stems from a mature cell wall, a process catalyzed by penicillin-binding proteins (PBPs) using their transglycosylase and transpeptidase activities, respectively [9]. Due to their important role in peptidoglycan synthesis, PBPs are good antibiotic targets, especially β-lactam antibiotics [10]. *Pseudomonas aeruginosa* codes for eight PBPs of which the PBP3 is the most essential for its growth as it exhibits transpeptidase activity needed to catalyze the linking of glycan subunits [11,12]. In *P. aeruginosa*, resistance against β-lactam antibiotics has been linked to the mutations in PBP3 and conditional mutations of PBP3 have been reported to cause cell division failures and lead to increased susceptibility to β-lactam antibiotics [11]. Overall, these reveal PBP3 as the most essential druggable target for the attenuation of resistance in *P. aeruginosa*.

Most recently, many strategies to counter AMR have been explored, with combination therapy being the most promising strategy to increase treatment efficacy and mitigate resistance development [13]. Over the years, drug development has focused on developing antibiotics mainly from microbial sources while paying less attention to plant-based antibiotics as potential alternatives [14]. However, in recent years, plant-derived compounds (especially phenolic acids – PAs) have gained great interest as alternatives to conventional drugs due to being more cost-effective, biocompatible and well-developed chemistry and biosynthetic pipelines which differ from microbe-derived products [15]. Higher plants and microbes utilize the shikimic acid (SA) pathway for bioproduction of secondary metabolites such as PAs, of which most of the plant derived PAs are produced through the SA pathway [16]. Plant-derived phenolic acids exhibit a wide range of biological activities such as antidiabetic, antioxidant, anticancer properties and notably, strong antimicrobial properties [17–19]. These compounds interact with transmembrane transporters for entry into the cell as opposed to the passive diffusion normally observed with conventional antibiotics. They also exert broader antimicrobial effects using a pleiotropic mechanism, where they act on multiple targets [20]. This highlights their greater potential as primary antimicrobial drug candidates in drug development and emphasizes their novel approach in dealing with AMR [21].

In novel antimicrobial identification and development, in silico methods have increasingly become invaluable tools in the identification of lead drug candidates, drug targets, and mechanisms of action [22]. Molecular dynamics (MD) simulation technique enables the examination of interactions between molecules (such as proteins and ligands), determination of the binding strength and energy of binding complexes, which are crucial for assessing the therapeutic potential of identified leads. In essence, it allows for the comprehension of the thermodynamic relationship between molecular systems (protein-ligand complex) and their behaviors over time [23–25]. On the other hand, molecular docking suffices as an advanced in silico tool for lead metabolites selection using their docking scores [26]. Despite ongoing efforts to curb the progression of drug resistance, it continues to escalate at a pace surpassing that of drug development, resulting in a decline in the effectiveness of most antibiotics [27]. In light of the foregoing, the SA pathway-derived PAs could prove to be promising leads for novel antibacterial development. Hence, this study explores PAs derived from

the shikimate pathway as *P. aeruginosa* PBP3 modulators using in silico analysis, complemented by *in vitro* evaluations to validate the antibacterial potential of the PAs either as stand-alone bioactive molecules or in combination with cefotaxime, a conventional antibiotic.

Methodology

In silico analyses

Acquisition and preparation of target protein and ligands

The penicillin-binding protein 3 (PBP3) 3D structure (3PBN) was obtained from the Protein Data Bank (https://www/rcsb.org/pdb), and prepared in UCSF Chimera 1.15 (water molecules, heteroatoms and nonstandard residues removed) followed by saving in 'pdb' format. Prior to performing molecular docking, the binding site grid coordinates were determined [28]. A total of 22 phenolic acids were selected for docking against PBP3. The PubChem compounds library (https://pubchem.ncbi.nlm.nih.gov/) was used in the retrieval of ligands 3D structures in 'sdf' format. The UCSF Chimera 1.15 software was then used to optimize and minimize all ligand structures by adding Gasteiger charges and H atoms. The ligands were thereafter saved as 'mol2' structures.

Docking of ligands to protein active site

Using UCSF Chimera with inbuilt AutoDock vina and default parameters, the PAs and antibiotic standard (cefotaxime) were docked into PBP3 active site using a grid corresponding to x-y-z (size: 43.2764/42.7334/39.8618 Å and center: 19.0477/-52.1288/20.7001 Å) coordinates. Complexes with the best binding poses and lowest docking scores were thereafter saved in pdb format and viewed using Discovery Studio 2021 to derive insights on interactions between ligands and active site residues. MD simulations proceeded using the phenolic acids with best binding affinity scores, as well as the standard [29].

Molecular dynamics (MD) simulation

The MDS was conducted on the Center for High Performance and Computing (CHPC) cluster using the AMBER 14 software and FF18SD force field variant. The ANTERCHAMBER ligands charges assignment aided the addition of chloride and sodium ions and TIP3P water molecules for system neutralization (cutoff was set at 8 Å for non-bond interactions). The Leap Module Shake algorithm was used to minimize the expansion of the chemical bonds involving hydrogen atoms, while trajectory processing for post-MDS analyses [including root-mean-square deviation (RMSD), root-mean-square fluctuation (RMSF) and radius of gyration (ROG)] was done via the CPPTRAJ program. The Molecular Mechanics/GB Surface Area method was used to determine binding free energies per complex during a 100 ns simulation time [30].

Chemical (quantum) reactivity determinations

The chemical reactivity and molecular attributes of the top-performing PAs were determined using Density Functional Theory (DFT)/B3LYP/631 G/+ basis set analysis [31] via the Gaussian 16 software. GaussView Version 6.0.16 was employed to view and visualize the results. Based on conceptual DFT (CDFT), the chemical descriptors (ionization energy, energy gap, softness, hardness, global electrophilicity, among others) that elaborate more on the molecular properties were calculated using the energies of frontier highest occupied molecular orbital (HOMO) and lowest unoccupied molecular orbital (LUMO) as foundation. These determinations consider the Koopmans theorem [32] and Parr and Pearson interpretation [33] of DFT.

Pharmacokinetic properties and drug-likeness prediction

The SwissADME online resource (https://www.swissadme.ch/index.php) was used to determine the pharmacokinetic, that is, absorption,

distribution, metabolism and excretion (ADME), and drug-likeness features of the top two phenolic acids and the cefotaxime positive control/standard [34]. The toxicity profiles of the lead compounds and the standard were evaluated using Protox-II (https://tox-new.charite.de/protox_II) webserver [35].

In vitro analyses

Bacterial culture standardization and antibacterial susceptibility test

In this study, *P. aeruginosa* ATCC 27,853 was used. Mueller–Hinton (MH) agar, nutrient agar and broth media were prepared using distilled water. The *P. aeruginosa* was subcultured onto fresh plates and incubated at 37°C for 24 h in before conducting *in vitro* tests. The stock culture was prepared by using the fresh plate to inoculate sterile normal saline (0.85%), followed by standardization (0.5 McFarland) of suspension to at 600 nm [108 CFU/mL inoculum size with optical density (OD) of 0.08]. Using the agar well diffusion method, 100 µL of standardized bacterial broth was spread under aseptic conditions on appropriately labeled Petri plates containing solidified Mueller Hinton (MH) agar. Then, 6 mm wells were borne into solidified plates, and about 50 µL aliquots of compound and standard at 200 mg/mL were aseptically transferred into respective labeled wells. Following adequate diffusion, plates were then inverted and placed in an incubator set at 37°C for 24 h. The diameter of the inhibition zone was then recorded in 'mm'. The assay was conducted in triplicates.

Microdilution assay

The broth microdilution technique described by Balouri et al. [36] was employed to determine the minimum inhibitory concentrations (MICs) of chlorogenic acid (CGA) and cefotaxime (CTX) against *P. aeruginosa*. In a 96-well microtiter plate, each well was filled with 50 µL Mueller–Hinton broth (MHB), followed by the addition of 100 µL two-fold serial dilutions of CGA and CTX, and 99.7% DMSO as a negative control. Subsequently, 50 µL of standardized bacterial inoculum was added into wells and the plate was allowed to incubate for 24 h at 37°C. Thereafter, the observed lowest concentration inhibiting bacterial growth (MIC) was recorded. In minimum bactericidal concentration (MBC) determination, 50 µl was taken from the well showing no turbidity/growth and transferred to MH agar plates which were then incubated under the same condition conditions as for MIC. The lowest concentration showing no viable growth after incubation was recorded as the MBC.

Synergy test (checkerboard assay)

The synergy of the combined treatments (CGA and CTX) was determined using the broth microdilution checkerboard assay. A two-fold serial dilution of CGA and CTX stock was done in a microtiter plate using 50 µL MH broth. Subsequently, 50 µL of standardized bacterial suspension was added, followed by the preparation of positive controls (single treatments of CGA and CTX), and then the plate was incubated for 24 h at 37°C. After incubation, the calculation of fractional inhibitory concentration index (FICI) helped to determine compound interaction type (synergism defined at $FICI \leq 0.5$, additive at $0.5 < FICI \leq 4$, and antagonism at FICI greater than 4) using the below formula:

FICI = (MIC of chlorogenic acid in combination/MIC of chlorogenic acid alone) + (MIC of cefotaxime in combination /MIC of cefotaxime alone). (1)

Time-kill kinetics

The killing rate of CGA, CTX and their combination against *P. aeruginosa* within a given contact time was determined using the broth microdilution technique [37]. In a 96-well microtiter plate, 50 µL of treatments (4 × MIC) was dispensed into each well containing 50 µL MH broth. Then, 50 µL of standardized bacterial inoculum was added to wells. The wells

containing only the bacterial suspension and MH broth served as the growth controls. The plate was incubated (37°C) and absorbance readings were taken at 600 nm every 2 h over 24 h period. The assay was conducted in triplicates.

Statistical analysis

Results were expressed as mean ± standard error of the mean (SEM) and statistical analyses were performed on Graph Pad Prism version 5.0 using non-parametric one-way analysis of variance tests to determine significance levels ($p < 0.05$).

Results and discussion

Molecular docking and amino acid residues interactions

Twenty-two phenolic acids and one FDA-approved drug (cefotaxime) underwent docking into the active site of the PBP3 receptor to assess their affinity to bind with the protein target, followed by lead identification. The results, detailed in Table S1 of the supplementary material, show the binding affinity of the phenolic acids as binding free energy (docking) score. Ideally, the greater the negative score, the stronger the binding, affinity and fitness for the protein. Of the 22 compounds, chlorogenic acid (CGA) and ellagic acid (EA) emerged with the most favorable binding affinity scores (−8.4 kcal/mol each) for PBP3 surpassing the standard drug, cefotaxime (CTX) (−7.5 kcal/mol). Study findings are in line with those reported by Sahare and Moon [12], where both CGA (−9.04 and −8.94 kcal/mol) and EA (−6.87 and −5.94 kcal/mol) had higher negative binding affinity than the control, methicillin (−6.47 and −4.33 kcal/mol) against the wild and mutated versions of PBP3. Collectively, these findings support the potential of these PAs as promising PBP3 modulators.

After docking, complexes formed by CGA, EA and standard, CTX, were analyzed via Discovery studio for their bond interactions with PBP3 active. The results are represented in Table 1 and Figure S1 of the supplementary material, from the observations it was revealed that there was a total of 18 interactions between CGA and PBP3. These included three conventional hydrogen bonds (Ser634, Tyr636), one C-H bond (Thr603), and one unfavorable bond interaction (Thr603) with bond lengths of less than 3Å, and several van der Waals. Additionally, multiple residues (ArgA428, SerA448, AsnA450, ProA660, LeuA663, ThrA619) engaged with CGA via Van der Waals bond. Ellagic acid, at the active site of PBP3, engaged with a total of 15 interactions, including 3 conventional hydrogen bond interactions (SerA392, ThrA621 and SerA429), one C-H bond (GluA620) with < 3 Å bond lengths (Table 1, Figure S2). The cefotaxime-PBP3 complex showed 18 total interactions [3 conventional hydrogen bonds (LysA427, SerA429, ThrA621), 2 C-H bonds (SerA448, ThrA603), sulfur-x (SerA429), pi-anion (GluA623)] with mean bond lengths ranging from 2.02 to 3.92 Å. Van der Waals interactions were observed with several residues (SerA392, LysA395, ArgA428, TyrA430, AsnA450, PheA454, GlnA524, among others) (Table 1, Figure S2). Notably, all the three compounds formed interactive bonds with key residues at the PBP3 protein active site, with observation of three conserved structural motifs of PBP3, SXXK (res 392–395), SXN (448–450), and KTG (618–620). Ser:392, in particular is important for the transpeptidation activity of PBP3, hence the interaction of CGA and EA with this residue may suggest their successful inhibition of PBP3 and this is an indication of binding successfully at the transpeptidase domain of PBP3 [28] (Figure S1-3).

Molecular docking techniques have a tendency of producing false-positive results of binding conformations, revealing them to be the most energy-minimized poses. To prevent this, a further validation protocol is normally done to ascertain the credibility and reliability of the docking technique. In this case, the root-mean square deviation (RMSD) measurement of the ligand

Table 1. Molecular interactions of lead compounds and cefotaxime with PBP3 target.

Ligands	Interactions (Bond distance Å)						
	Hydrogen Bond (Distance)	Carbon-Hydrogen Bond	Unfavourable donor-donor, acceptor	Pi-sigma, alkyl/ Amide Pi stacked	Sulphur X	Pi Cation & Anion	Van der Waals
Cefotaxime	Lys427 (2.02), Ser429 (2.79) Thr621 (3.53)	Thr603 (2.94) Ser448 (3.33)	-	–	Ser429 (3.14)	Glu623 (3.93)	Ser392, Phe454, Arg428, Gln524, Asn450, Thr619, Pro661, Tyr430, Lys395, Pro660
Chlorogenic acid	Ser634 (2.73 & 2.57), Tyr636 (2.57)	Thr603 (2.41)	Thr603 (2.71)	–		–	Ser392, Ser429, Arg428, Ser448, Asn450, Val606, Leu663, Thr635, Gly620, Thr621, Thr619, Pro660
Ellagic acid	Ser429 (1.96), Thr621 (2.11), Ser392 (2.38)	Gly620 (2.43)	–	–		–	Pro660, Val606, Thr603, Thr619, Ser448, Tyr430, Asn450, Ser449, Arg428, Lys395

from its point of reference in the resulting complex is used to confirm the accuracy of the docking geometry [38]. An RMSD value of <1 between docked ligand and the resulting complex is set as the acceptable cutoff value that implies the similar binding orientation, which in turn validates the docking technique as being one without error [39]. In this study, the docking validation via the superimposition approach showed the top-two docked compounds as having similar binding orientation as the native ligand with an RMSD value of approximately 0.5 Å (Figure 1) and excellent display of the gatekeeper residue (Ser392) agrees with a previous study [40].

Structural dynamics of the ligand-protein complexed systems

Molecular docking only serves as an initial indicator of a compound's affinity for a target, and as such the intrinsic information on the stability of their resulting interactions remains unknown [41]. Therefore, best-posed complexes of hit compounds and the standard were further put through a 100 ns MD simulation to assess the impact of ligand binding on the protein target, PBP3, followed by binding free energy and post-trajectory determinations [42]. The calculated binding free energies are presented in Table 2 and revealed that CGA (−33.65 Kcal/mol) had the least binding free energy (ΔGbind) score relative to the standard (−30.10 Kcal/mol) and EA (−18.14 Kcal/mol). As such, a better interaction was observed between the CGA-PBP3 complex which translates to greater stability [29]. This finding is in line with the docking scores which revealed CGA as being more fit for the target's binding pocket over CTX. However, this was quite an interesting observation considering that both CGA and EA exhibited the same fitness in docking scores. Overall, the results accentuate the significance of conducting MD simulation to help ascertain the docking results in the search for lead drug candidates for drug development [43].

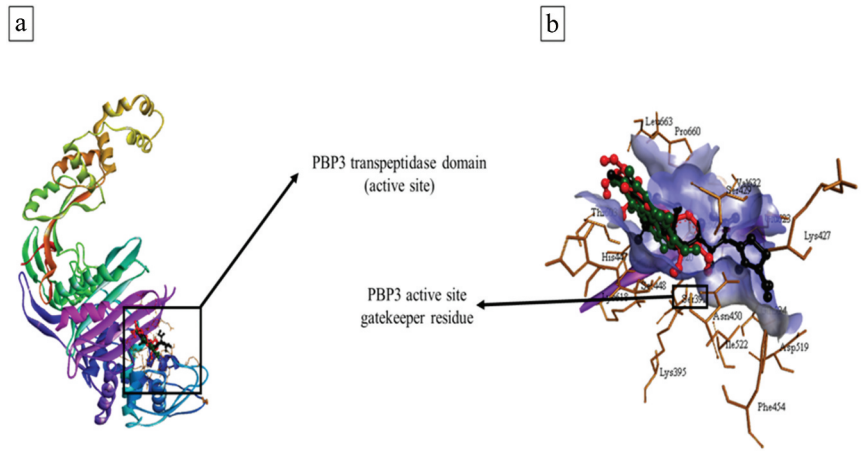

Figure 1. The 3D (a) and 2D (b) representations of docking validation showing superimposition (with a low RMSD value of 0.5 Å) of the top-two phenolic acids, chlorogenic acid (red) and ellagic acid (green) assuming a similar orientation to the native ligand, cefotaxime (black) at the active site showing the gatekeeper residue (Ser392).

Table 2. Thermodynamic profiles of hit phenolic acids and standard complexes.

	Energy components (kcal/mol				
Complex	ΔE_{vdW}	ΔE_{elec}	ΔG_{gas}	ΔG_{solv}	ΔG_{bind}
CTX+ PBP3	−42.20 ± 6.06	−47.28 ± 13.35	−89.48 ± 9.85	59.37 ± 9.50	−30.10 ± 4.60
CGA+ PBP3	−37.77 ± 4.10	−47.73 ± 14.88	−85.51 ± 14.69	51.86 ±10.74	−33.65 ± 5.52
EA+ PBP3	−28.06 ± 3.23	−8.09 ± 8.77	−36.15 ± 8.90	18.01 ± 5.59	−18.14 ± 4.16

PBP3: penicillin-binding protein 3, ΔEvdW: van der Waals energy, ΔEelec: electrostatic energy, ΔGgas: gas-phase free energy, ΔGsolv: solvation energy, ΔGbind: total binding free energy, CTX: cefotaxime, CGA: chlorogenic acid, EA: ellagic acid.

PBP3: penicillin-binding protein 3, RMSD: root-mean-square deviation, RMSF: root-mean-square fluctuation, RoG: radius of gyration, SASA: solvent accessible surface area, CTX: cefotaxime, CGA: chlorogenic acid, EA: ellagic acid.

The post-MD trajectory, the root-mean square-deviation (RMSD) parameter indicates the degree of stability within a protein-ligand complex and accounts for changes in the apo-protein structure due to compound binding. A lower RMSD value indicates greater stability of the complex [44]. The RMSD data obtained for the top two compounds and the control after the 100 ns simulation are represented in Figure 2a and Table 3. The CGA-PBP3 (4.18 Å) complex had the lowest RMSD value compared to apo PBP3 (4.22 Å) and the CTX (5.00 Å) and EA (5.81 Å) complexes with PBP3. A convergence within all systems was noted at 5 ns from where the complexes stabilized as they fluctuated between 2–8 Å till the simulation period ended (Figure 2a). From these observations, all the complexes' RMSD values including that of the apo structure were over the benchmark of 3.0 Å Ramirez et al. [45]. However, due to the RMSD values of CGA and apo PBP3 being non-significantly different, both CGA and apo PBP3 stimulate a comparable degree of stability although still in favor of GCA due to the marginal difference in RMSD value and the fact that CCA outcompetes CTX, a standard drug in stimulation more structural stability further highlights its prospect as a lead and potential modulator of PBP3.

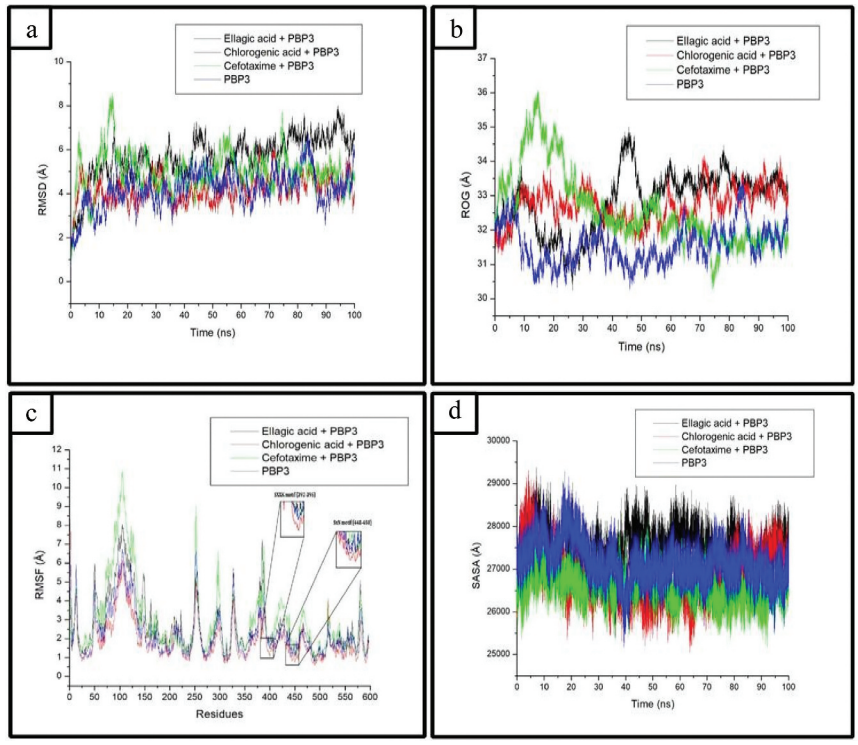

Figure 2. Comparative MD simulation plots of the PBP3 complexes formed by the top two compounds and standard over 100 ns period. (a) Root-mean square deviation (RMSD), (b) radius of gyration (RoG), (c) Root-mean square fluctuation (RMSF) and (d) solvent accessible surface area (SASA).

Table 3. Post-MD simulation attributes of top two compounds and standard-PBP3 complexes.

		Average (Å)		
Complex	RMSD	RMSF	RoG	SASA
CTX + PBP3	5.00 ± 0.90	2.93 ± 1.86	32.58 ± 1.09	26634 ± 358
CGA + PBP3	4.18 ± 0.60	1.92 ± 1.09	32.75 ± 0.48	26932 ± 552
EA + PBP3	5.81 ± 1.08	2.61 ± 1.45	33.06 ± 0.90	27535 ± 421
PBP3	4.22 ± 0.83	2.25 ± 1.22	31.56 ± 0.56	27151 ± 473

During the simulation, fluctuations within the CTX and EA complexes with PBP3 were observed, these fluctuations are indicative of the ligands' instability within the protein's binding pocket as they move around in an attempt to find a more favorable binding pose prior to reaching a stable. This means that the protein's structure undergoes alterations due to new interactions being formed. Similar to RMSD, the radius of gyration (ROG) parameter measures the extent of compactness of a protein after ligand binding and relates it to the stability of the complex, a lower ROG value means that better stability will be achieved within the protein structure [46]. In this study, the findings revealed the ROG values of the compounds and apo structure to be as follows: CCA (32.75 Å), EA (33.06 Å), CTX (32.58 Å) and apo PBP3 (31.56 Å) (Figure 2b and Table 3). We found that the compounds' ROG values were comparable to those of the CTX and apo-protein, while CGA

and EA compete favorably with CTX and bring about a similar degree of compactness within PBP3.

On the other hand, the RMSF descriptor measures the structural flexibility of amino acid residues in the binding pocket of a protein and can also help in discerning the degree of stability. Fewer fluctuations relate to more stable bond interactions and less movement [47]. A low RMSF value relates to a more structurally stable and less flexible active site [41]. From the observations, the RMSF values of CGA, EA and CTX were 1.92 Å, 2.61 Å, and 2.93 Å, respectively, while that of the apo PBP3 was recorded as 2.25 Å (Table 3). Unlike the RMSD values, these values were well within the limits of ˂3.0 Å (Ramirez *et al*., 2018). Once again, these findings correlate with those of RMSD that prove that CGA is the most prominent ligand which brings about more stability compared to EA and CTX. This is supported by its low RMSF value showing fewer amino acid residues flux/movement at the active site upon binding. The reverse was the case with EA and CTX, same as with their ROG where more fluctuations was observed, indicating instability and less compactness compared to CGA. This outcome accentuates the potential of CGA as a potential therapeutic. Our findings align with those of a previous study where a phenolic compound-alpha amylase complex showed lower RMSF score, indicating a well-structured and stable system [30]. Most importantly, CGA binding to PBP3 significantly stabilized the movement of residues much more than CTX, EA, and the apo structure (Figure 1c). This could be confirmed by noting the movements of the active site residues at two of the three structural motifs, SXXK (392–395 residues) and SXN (448–450 residues) motifs. At these regions, the fluctuations observed with CGA are minimal relative to those of CTX and EA.

An analysis of SASA scores was used to show changes in a surface area accessible to immediate solvent molecules due to ligand binding and to study the effects on protein folding, more structural stability is achieved with a low SASA value, while the reverse denotes reduced complex system stability and surface area increase [44]. In the results depicted in Table 3 and graphically portrayed in Figure 1d, the SASA values for CGA, EA and CTX complexes were 26,932.40 Å, 27535.68 Å, and 26,634.83 Å, respectively, while the apo-PBP3 exhibited a SASA value of 27,151.35 Å. The high SASA values of the apo PBP3 and EA indicate a more increased surface area and thus more exposure to water which leads to compromised stability. However, CGA and CTX upon binding to PBP3 induce a change within the protein structure that is enough to slightly decrease the accessible surface area in such a manner that they get buried within the active site of PBP3 and experience fewer disturbances from the outside environment. Thus, they achieve more stability. Since CGA competes with CTX favorably, this proves its stance as a promising PBP3 modulator.

Hydrogen bonding assumes a vital role in protein–ligand interactions contributing to the stability of the complexes and influencing the binding free energy of the system, as highlighted by Chen et al. [48]. Therefore, this study also explores this parameter of protein-ligand systems. The complexes' intermolecular hydrogen bonds are represented in Figure 3a-c, which show the presence of stable H-bonds formed within the complexes, which persist throughout the simulation, fluctuating between 16.6 and 18.8 H-Bonds. This suggests that CGA and EA effectively form and maintain strong and stable interactions with the binding pocket of PBP3 that is comparable to the standard, CTX. Notably, Kumar et al. [49] reported similar findings where sesame seed-derived phytochemicals were evaluated against the main protease (M^{pro}) of SARS CoV-2. In their research, the metabolites consistently formed three to four hydrogen bonds in all complexes, underscoring their firm interaction with the M^{pro} active site and the resulting stability of the complexes.

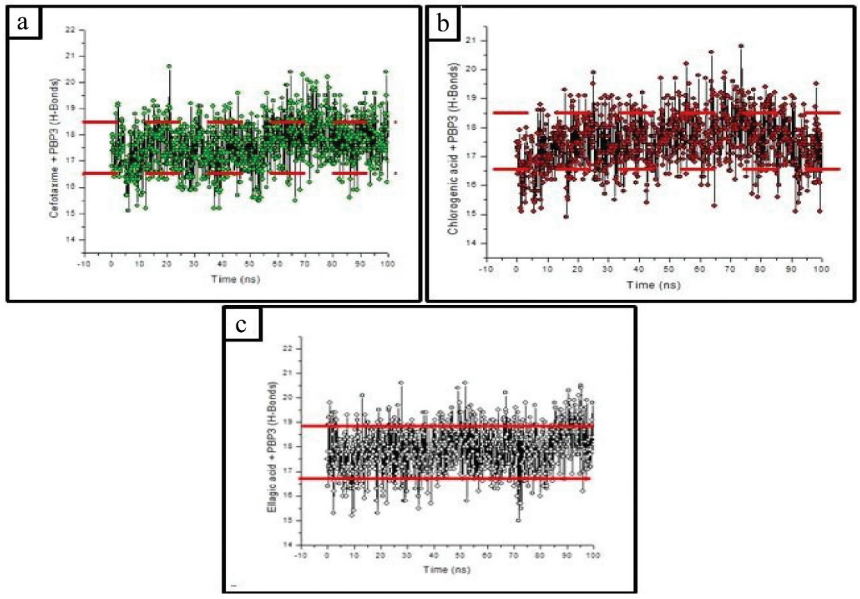

Figure 3. Hydrogen bonds formed over a 100 ns simulation period. (a) cefotaxime, (b) chlorogenic acid, and (c) ellagic acid, against PBP3.

After conducting the MD simulation, snapshots of the complexes at 100 ns were generated to assess the changes in interactions between the hit compounds and amino acid residues at PBP3 active site. The snapshots are depicted in Figures 4a-c and reveal that all compounds formed new interactions different from those seen before the MD simulation. Similar to the interactions seen after docking, there is still a presence of hydrogen bonds, van der Waals forces, and pi- and alkyl interactions. All these interactions, especially hydrogen bonds and van der Waal interaction, are key components that facilitate ligand binding, influence binding free energy and tremendously contribute to the stability of protein-ligand systems [48]. Cefotaxime, chlorogenic acid and ellagic acid exhibited diverse interactions with PBP3's active site with varying degrees and numbers. For instance, 29 interactions were observed for CTX [7 conventional H-bonds (Ser403, Gln479, Thr558, Thr574, Glu578), 1 pi-anion interaction (Glu578), 8 C-H bonds, 1 alkyl bond (Pro613), 11 van der Waals] as illustrated in Figure 4a.

About 20 total interactions were observed for the chlorogenic acid-PBP3 complex [6 conventional H-bonds, 3 C-H bonds (Thr576, Ser384, Gly575), 1 pi-pi T-shaped (Phe386), 1 pi-alkyl bond (Pro613), 1 amide pi-stacked bond (Ser384), 8 van der Waals bond interactions] (Figure 4b). Ellagic acid, on the other hand, engaged in 14 interactions with the PBP3 active site, a difference of 15 interactions from the standard, CTX and six interactions less than CGA (Figure 4c). Comparatively, CTX had a higher number of overall interactions (including H, van der Waals bonds) than CGA and EA. Despite this, CGA against PBP3 had the highest binding free energy compared to CTX and EA. Hence the interactions at 100 ns partially contributed to its total ΔG_{bind} and do not entirely dictate which compound would perform better as the ΔG_{bind} sums up ligand–protein interactions throughout the simulation. Tallei et al. [50] previously highlighted in their study that a higher number of hydrogen bonds with a single amino acid residue could decrease the binding free energy score while strengthening the stability. This may explain why CTX has

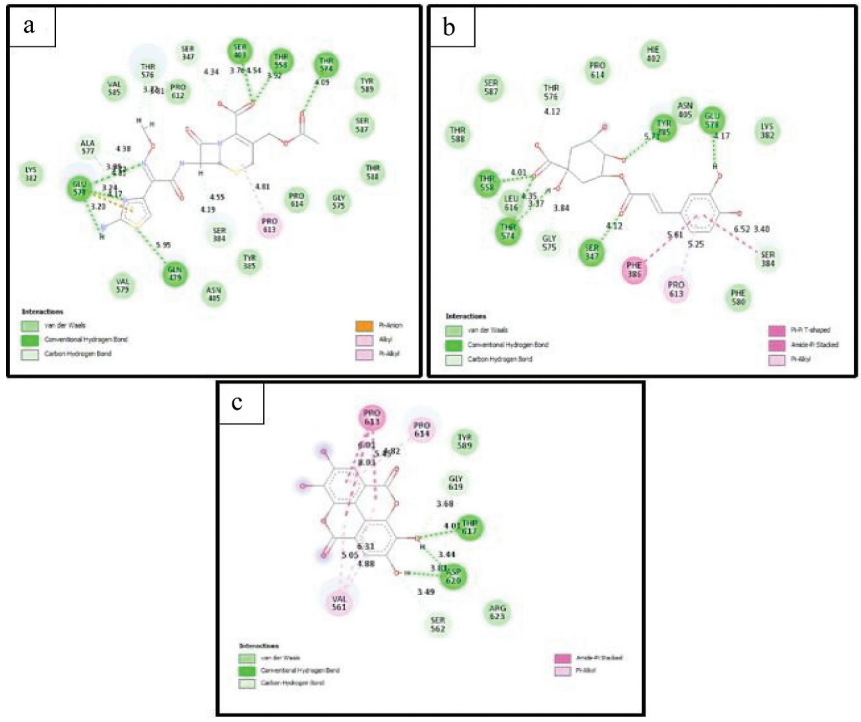

Figure 4. Intermolecular interactions formed at 100 ns MD simulation of ligand-protein complexes. (a) cefotaxime, (b) chlorogenic acid and (c) ellagic acid, against PBP3.

a low binding free energy despite having more H-bonds. Again, the residue, GluA578 interacted with CTX via numerous H-bonds, while SerA384, SerA403, ThrA576 formed multiple C-H bonds, potentially contributing to the decreased ΔG_{bind}. Notably, the ΔG_{bind} observed for EA may be attributed to the lack of H-bonds, van der Waals and fewer interactions compared to its counterparts. Additionally, pi interactive bonds serve as facilitators of protein folding and intercalators and stabilize ligands at the protein active site. Their interactions could have contributed to the decreased binding affinity energy [51,52].

The density functional theory (DFT) analysis was conducted for the top-performing compounds to shed light on their molecular properties (Table 4, Figure 5). The Highest Occupied

Table 4. Conceptual density functional theory (CDFT) of the top three metabolites.

CDFT parameters (eV)	CGA	EA	CTX
E_LUMO	−2.0557	−2.27036	−2.07673
E_HOMO	−6.08489	−6.47107	−5.73531
Energy gap (ΔE)	4.029192	4.200705	3.658582
Ionization energy (I)	6.084891	6.471068	5.73531
Electron affinity (A)	2.055699	2.270363	2.07673
Hardness (η)	2.014596	2.100352	1.829291
Softness (S)	0.496377	0.476111	0.54666
Electronegativity (χ)	4.070295	4.370716	3.906019
Chemical potential (μ)	−4.07029	−4.37072	−3.90602
Electrophilicity index (ω)	4.111817	4.547608	4.170192

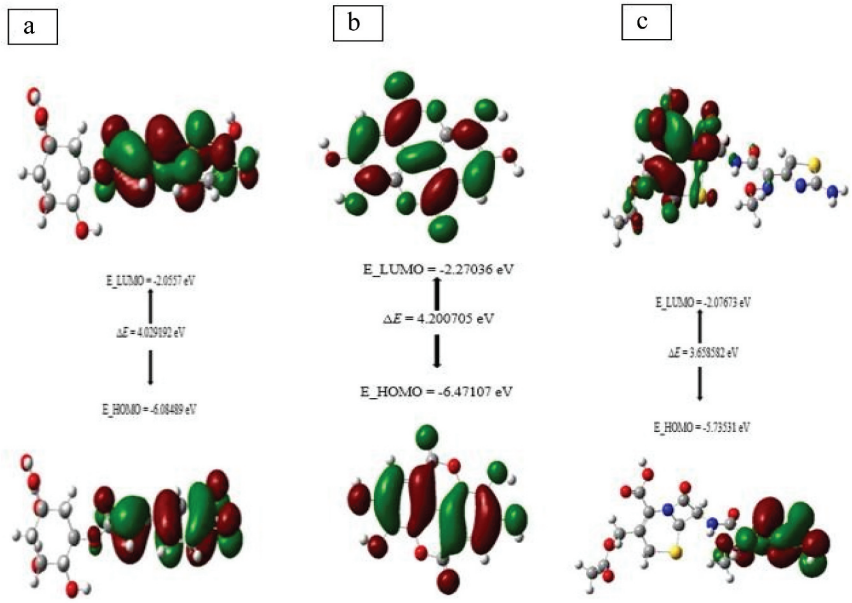

Figure 5. The associated transition energies and frontier molecular orbitals for (a) chlorogenic acid, (b) ellagic acid and (c) cefotaxime.

Molecular Orbital (HOMO) and Lowest Unoccupied Molecular Orbital (LUMO) parameters or critical factors help to determine system chemical reactivity profile [53] and mechanism of action of promising therapeutic compounds [54]. The HOMO orbital energy indicates the donating potential of a compound and is proportional to the compound's ionization energy, while LUMO describes the energy-withdrawing tendency of a compound together with the electron affinity descriptor [55]. The energy gap informs on the chemical reactivity and stability of a compound, with a lower energy gap revealing an unstable state while high reactivity implies molecule softness [56]. Results showed that CTX had the lowest energy gap followed by CGA. This could be accounted for by their higher affinity (high binding energy) for PBP3.

Ellagic acid had the highest energy gap among the three molecules suggesting higher stability and less reactivity, which could have been influenced by its low affinity for PBP3. Also, the binding of the reference standard and CGA significantly decreased the accessible surface area of the protein, while the binding of EA increased the accessible area. This finding may indicate the low thermodynamic suitability of EA with PBP3. These results are consistent with the findings of Ma et al. [57] where lower energy gaps were observed for amentoflavone and hinokiflavone, which exhibited high binding free energy against SARS-CoV-2 main protease (Mpro). The ionization energy of a molecule defines the amount of energy needed to separate an electron from an atom and electron affinity speaks more on the energy that is needed to accept an electron. Lower ionization is associated with higher reactivity that translates to an unstable compound and provides information about the inhibition of a molecule.

Contrary to this, a higher electron affinity indicates a superior electron-withdrawing ability of a compound [55]. As observed in Table 4, the standard had the lowest ionization energy, but upon comparison, CGA had the lowest ionization potential compared to

EA, suggesting its higher reactivity and high inhibition power. These findings agree with the higher binding free energies of CGA and CTX complexed with PBP3 compared to the lower binding free energy of EA. In contrast to these findings, EA has a high electron-withdrawing ability as it has a higher electron affinity and is more stable. This finding is consistent with the high energy gap and ionization potential of EA. The CTX displayed the lowest hardness followed by CGA and EA. A higher softness value was observed in the same fashion. A molecule's softness and hardness also speak to its chemical reactivity and stability. The low hardness and high softness values connote more reactivity and low stability [58]. Findings show that CGA is the most reactive or less stable after the standard which agrees with the low energy gap value, ionization potential energy and higher binding affinity of CGA.

The electronegativity and chemical potential quantify the capability of an atom or functional group to attract electrons. The results in Table 4 indicates that EA has the highest capacity to bond electrons, while CGA and CTX had a low electronegativity value. This shows a low ability to attract electrons and describes their low stability as they easily lose electrons. This is also supported by their low ionization energy and low electron affinity. For EA, these findings again speak on its chemical stability, as a greater electronegativity denotes higher stabilization and means it likely forms bonds with high bond strength. The electrophilicity index defines the electron withdrawing ability of a compound in response to an electron from the outside environment. A higher electrophilicity index value indicates a good electrophile, while a lower value describes a reactive nucleophile [55]. Taking from the results in Table 4, EA clearly showed a great electrophilicity index (good electrophile) which was consistent with the electronegativity value. Chlorogenic acid and CTX displayed a low electrophilicity value compared to EA (reactive nucleophiles) which was consistent with other descriptors and indicated the higher reactivity of both CGA and CTX. Overall, CGA is the most active phenolic acid, other than the standard, attesting to its potential as a modulator of PBP3.

CTX: cefotaxime, CGA: chlorogenic acid, EA: ellagic acid.

Pharmacokinetic properties prediction of the lead compounds

Assessing the pharmacokinetic, drug-likeness and toxicity attributes of a compound serves as a preliminary indication of how the body interacts with an administered drug during the period of exposure and allows one to discern the compound's *in vivo* medicinal friendliness. These data give some degree of confidence in a compound's potential as a therapeutic agent while aiding in decreasing the chances of the drug's failure during pre- and clinical trials in drug development [59,60]. The top two identified compounds, CGA and EA against PBP3 exhibited fairly good pharmacokinetic properties with 0–1 violations (within acceptable limits) of the Ro5. They both had a molecular weight $<$ 500 g/mol, lipophilicity (LogP) values of $<$ 5 [CGA (0.94), EA (0.79)], and hydrogen bond acceptors of $<$ 10 [CGA (9), EA (8)]. The reference standard also exhibited good results with only one violation of the Ro5 (HBA$>$10) (Table 5). As all the compounds including the standard passed the Ro5, this may be indicative of their ability to progress through the systemic circulation and reach the target sites while still maintaining the relevant concentrations to bring about their therapeutic effects [61].

Lipophilicity is a crucial drug property in drug design which not only influences drug uptake, distribution and metabolism but also encourages off-target binding with increased values. It also dictates how a drug should be formulated and its dosage [62]. All the evaluated

Table 5. The pharmacokinetic attributes of lead phenolic acids and cefotaxime.

Property	Cefotaxime	Chlorogenic acid	Ellagic acid
Molecular weight (≤500 g/mol)	455.47	354.31	302.19
H-Bond acceptor (≤10)	12	9	8
H-Bond donor (≤5)	4	6	4
Water solubility	Very soluble	Very soluble	Soluble
Lipophilicity (LogP ≤5)	2.05	0.96	0.79
GIT absorption	Low	Low	Low
Bioavailability score	0.11	0.11	0.55
BBB permeability	No	No	No
P-gp substrate	No	No	No
CYP1A2 inhibitor	No	No	Yes
CYP2C19 inhibitor	No	No	No
CYP2C9 inhibitor	No	No	No
CYP2D6 inhibitor	No	No	No
CYP3A4 inhibitor	No	No	No
CYP3A4 substrate	Yes	Yes	No
Acute oral toxicity class	6	5	4
Carcinogenicity	Inactive	Inactive	Active
Hepatoxicity	Inactive	Inactive	Inactive
Mutagenicity	Inactive	Inactive	Inactive
Cytotoxicity	Inactive	Inactive	Inactive
Immunotoxicity	Inactive	Active	Inactive
Lipinski's rule[50]	Yes (1 violation: HBA˃10)	Yes (1 violation: HBD˃5)	Yes (0 violation)

compounds in this study did not exceed the set benchmark of 5, suggesting their lipophilic nature. This is a crucial property needed to have good absorption. It also indicates an ability to penetrate the lipid bilayer of cellular membranes, be distributed successfully *in vivo* and reach their target sites. This also means that the compounds are not highly lipophilic, thus limiting the chances of off-target binding and consequently less toxicity [63]. Interestingly, both the compounds are soluble in water, with CGA being the most soluble and easier to transport through the bloodstream than EA. Again, since both CGA and CTX are very soluble in water, it accentuates the potential of CGA as a good therapeutic agent because it competes favorably with an established commercial drug.

GIT: Gastrointestinal tract, BBB: Blood–brain barrier, CYP: Cytochrome P450.

The gastrointestinal tract (GIT) assumes a very crucial role in drug absorption of orally administered drugs [64]. As such, it is of great significance to evaluate such factors (GI absorption) so as to determine their effect on plasma concentration of oral medications and residence time at the absorption site. The observations showed that both lead PAs and the standard had low GIT absorption (Table 5) which could be due to elevated gastric emptying, intestinal motility, and unsuitable gut pH for optimum absorption [65]. In another sense, this may indicate their preference for an alternative route of administration over oral administration. Both CTX and CGA exhibited a low bioavailability score of 0.11 each, suggestive of their limited time in the GIT tract, and their low GIT absorption influences their bioavailability regardless of their high solubility in water. Contrary to this, EA had a favorable 0.55 bioavailability score (Table 5), suggesting its suitability for oral administration and less quantities required to exert the expected pharmacological effects, In the case of CGA and CTX, a change in route of administration may yield a more favorable bioavailability score [41,66]. The blood–brain barrier (BBB) is a selective semi-permeable membrane that blocks most drugs and pathogens in the blood from entering the brain and aids in the regulation of the microenvironment of the

central nervous system (CNS) [67]. All three compounds could not penetrate the BBB, an advantageous observation since these compounds are not intended to be used as treatments for neurological diseases that require penetrating the BBB to reach their target site (CNS). This generally means there is no risk of neurotoxicity when they are administered.

Furthermore, CGA and CTX did not inhibit the clinically important cytochrome P450 (CYP450) isoenzymes which are crucial enzymes partaking in drug metabolism and detoxification of foreign chemicals within the human body [10]. This finding accentuates their superiority over EA in not causing drug toxicity due to the malfunctioning of the CYP enzymes as a result of inhibition. Only EA showed inhibition of CYP1A2 (Table 5), suggesting a high possibility of resulting in unfavorable drug–drug interaction compared to the other two compounds. Although CYP1A2 is not the most important within the CYP450 family, it still plays a significant role in drug metabolism and cannot be overlooked. Since half the metabolism in the human liver is under the control of CYP3A enzymes and most commercial drugs' metabolism is due to CYP3A4, it would seem that CGA and CTX also have affinity for this isoenzyme while EA does not. Findings have shown that the co-administering CGA and CTX may likely not result in unfavorable reactions. However, this claim was further validated by directly docking the said compounds against the CYP3A4 isoenzyme active site with ketoconazole (inhibitor) and rifampicin (inducer) serving as the controls. The outcome was in line with the previous claim as CGA (−9.0 kcal/mol) and CTX (−7.3 kcal/mol) exhibited docking scores that were less than those of the ketoconazole (−9.6 kcal) and rifampicin (−9.4 kcal/mol) (Table S2).

Toxicity is a major limiting factor that influences the development and usage of new compounds or drugs as therapeutic agents, hence for drug development, it is important to ascertain their toxicity levels [68–70]. Therefore, in this study, the toxicity profiles of the three compounds were evaluated. Both CGA and EA were found to be active for at least one of the toxicity endpoints, immunotoxicity and carcinogenicity, respectively (Table 5). This means that these compounds are likely to induce adverse side effects on the immune system and trigger cancer upon ingestion at high concentrations. However, these are areas that could be rectified by modifying the structures of these compounds to improve their toxicity profiles [71,72]. The standard, CTX was found to be inactive for all toxicity endpoints. This may be suggestive of its modification as it is already a commercialized drug. These findings also reveal the need to modify the structures of CGA and EA to further improve their pharmacokinetic and toxicity profiles. The predicted lethal dose (LD_{50}) of CGA and EA were 5000 mg/kg (class V) and 2991 mg/kg (class IV), respectively, while CTX had an LD_{50} of 20,000 mg/kg (class VI). Based on the LD_{50} values, it is evident that CGA stands a better chance of being utilized as a therapeutic than EA which is categorized in class 4, with a higher lethality profile [35]. It is also quite important to understand that the overall toxicity of a drug may be influenced by other factors aside from the chemical structure such as lifestyle, life stage, rate of metabolism, genetics, route of administration, overall health status and dosage [73]. Taken together with the thermodynamic profile results (Table 3), the overall results support CGA as the more promising compound and potential PBP3 modulator relative to EA and CTX.

In vitro analyses

The antimicrobial potential of CGA and CTX were evaluated against *P. aeruginosa* to validate the computational findings, and the results are presented in Table 6. Both compounds showed antimicrobial activity [CGA (23 mm inhibition zone, MIC of 200 mg/mL) and CTX (29 mm inhibition zone, MIC of 0.8 mg/mL)], although CTX was the most active

Table 6. *In vitro* antibacterial activity of chlorogenic acid and cefotaxime.

	Zone of inhibition (mm)		MIC (mg/mL)		MBC (mg/mL)	
Isolate	CTX	CGA	CTX	CGA	CTX	CGA
P. aeruginosa ATCC 27,853	29±0.1	23±0.2	0.8	200	3.2	800

since lesser concentrations were needed to inhibit *P. aeruginosa* growth in comparison with CGA. This may be linked to CGA's limited diffusion into the assay medium. However, CGA also exhibited a significant antimicrobial effect. Again, as a standard drug CTX's activity may have been boosted by its modifications which enhanced its antibacterial action relative to CGA used in its unmodified form. The findings support *in-silico* toxicity outcomes where CTX was nontoxic at all toxicity endpoints. Higher antibacterial concentrations for CGA relative to the standard antibiotic have also been reported in an earlier study using PAs against Gram-positive, *P. aeruginosa* and other Gram-negative microbes where MICs fell within 500–2000 mg/mL [74]. Yet the reverse was the case in another study where CGA MIC against several Gram-positive and Gram-negative microbes (excluding *P. aeruginosa*) showed a 0.02 to 0.08 mg/mL range [75], suggesting strain-dependent susceptibility may play a key role.

CTX: Cefotaxime; CGA: chlorogenic acid; MIC: minimum inhibitory concentration; MBC: minimum bactericidal concentration

Combination therapy has been extensively studied and used as a means of enhancing the potency of drugs and averting drug resistance during treatment [76]. As such, in this study, the synergistic (combined) effect of chlorogenic acid and cefotaxime against the test organism, *P. aeruginosa* was evaluated using the checkerboard microdilution method, and the findings of their combined effect are presented in Table 7. The checkerboard method allows one to distinguish the type of drug interaction or effect when two or more drugs are combined, such interactions include positive (additive and synergistic) and negative (antagonistic) combined effects [77]. The concentrations used in the combination for CGA varied between 1/256 × MIC to 4 × MIC while those of CTX varied between 1/32 × MIC to 2 × MIC. Based on the findings bacterial growth inhibition was observed at the lower combined concentrations of 50 mg/mL (CGA) and 0.2 mg/mL (CTX), and at 25 mg/mL (CGA) and 0.4 mg/mL (CTX), where the FICI value of the former resulted in 0.5, which corresponds to a synergistic interaction and the latter had a FICI value 0.625 relating to an additive effect (Table 7). The synergistic effect observed at lower concentrations than their respective MICs highlights the ability of CGA to enhance the activity of CTX thus allowing it to exert an increased effect (at low concentration) that is greater than when given separately, and this interaction resulted in a four-fold reduction in MIC value, this observation is in line with literature, where such a fold decrease stems from a synergistic interaction [78]. It should also be appreciated that such an interaction may also point to these two compounds having different mechanisms of action rather than targeting the same target [79]. The additive effect observed signifies that the addition of CGA at that specific concentration does not alter the degree of therapeutic

Table 7. Inhibition and interaction effects of chlorogenic acid and cefotaxime combination.

Isolate	Treatment	MIC_a (mg/mL)	MIC_c (mg/mL)	FICI	Interaction
Pseudomonas aeruginosa ATCC 27,853	Chlorogenic acid + cefotaxime	CGA (200) CTX (0.8)	CGA (50) CTX (0.2)	0.500	Synergistic
			CGA (25) CTX (0.4)	0.625	Additive

effect of CTX but rather may reduce its side effects. However, drug combinations with such interactions are highly unrecommended as they have a prevalence of causing adverse side effects [80]. In a nutshell, CGA facilitates a reduction in the minimum dose required for effective antimicrobial activity and thus has the potential to limit the possibility of side effects. However, for actual implementation as a therapeutic agent, further studies are warranted to gain insight into the exact mechanism of the antibacterial action of CGA against *P. aeruginosa*, as well as to understand the mechanism behind their combined interaction.

MIC_a: Alone; MIC_c: Combination CTX: cefotaxime; CGA: chlorogenic acid; FICI: fractional inhibitory concentration index.

The time-kill kinetics of the test organism by chlorogenic acid and cefotaxime is presented in terms of changes in the optical density of viable cells at 600 nm shown in Figure 6. This assay makes it possible to gauge the rate at which the treatments' cidal activity occurs [81]. The treatments, chlorogenic acid, and cefotaxime exhibited a bacteriostatic effect at 4 × MIC (800 mg/mL and 3.2 mg/mL, respectively) against the test bacteria, the same trend was observed with the combination of both treatments at the same concentrations, this conclusion was drawn following the observation that the treatments did not manage to reduce 99% of the viable cells within 24 h experimental period, hence the bacteriostatic effect. However, it should be appreciated that all the treatments exhibited a significant steady decrease in the population of the test bacteria as evidenced by the reduction in optical density at each interval between 0 and 10 h. This observation is suggestive of the potential therapeutic effect of the treatments. An increase in optical density, which correlates to the regrowth of bacterial cells, was observed after 10 h, hence the bacteriostatic effect mentioned earlier. This shows a concentration-dependent killing and the increase in populations could also be attributed to the saturation and depletion of the treatments after a certain period of time, which allows persistent cells to reproduce and replenish populations due to the absence of antimicrobial pressure. According to Gregoire et al.

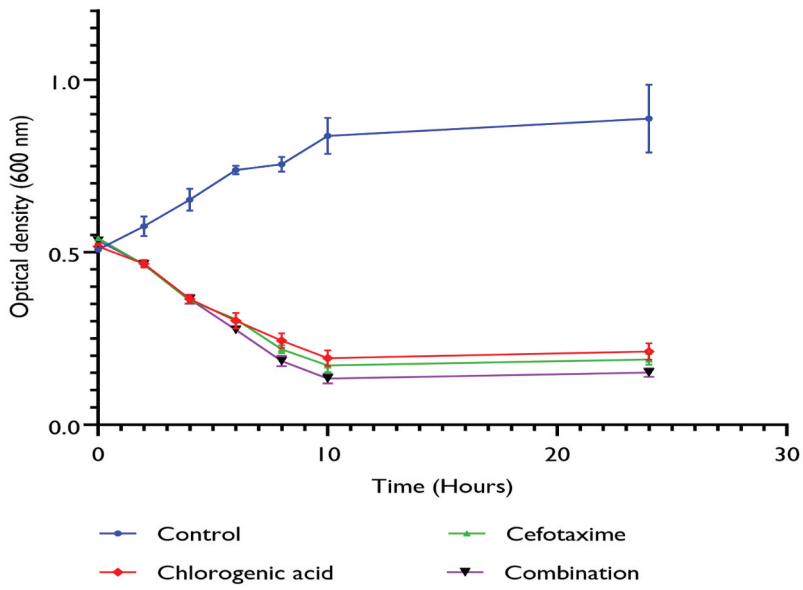

Figure 6. Time-kill growth curve of top compounds alone and in combination with standard antibiotic at 4×MIC against *P. aeruginosa* ATCC 27,853.

[82], the regrowth of bacterial subpopulations post-treatment exposure could be interpreted as models of development of drug resistance. The observations from this study are in agreement with the findings of Basri et al. [37] where the exposure of resistant Staphylococcus aureus (HUKM strain) to ε-viniferin and vancomycin and their combination resulted in regrowth after 6 h and continued through to 24 h.

Conclusion

This study explored 22-shikimate pathway-derived phenolic acids (PAs) for their affinity for the active site of *P. aeruginosa* PBP3, with chlorogenic and ellagic acid emerging as the lead compounds with the best binding affinity, surpassing that of the reference drug, cefotaxime. They interacted with the catalytically important residues constituting the three conserved structural motifs, SXXK, SXN and KTG, especially Ser392, which interacts with the natural substrate of PBP3 during crosslinking of glycan subunits, thus indicating potential inhibition of PBP3. Thermodynamic stability assessment revealed chlorogenic acid as the superior inhibitor compared to ellagic acid. Low fluctuations at the SXXK motif (Ser392) for all the complexes revealed the successful binding and blocking of the Ser392 and inhibition of the protein. The electronic properties assessment highlighted chlorogenic acid and cefotaxime as the most reactive, reinforcing chlorogenic acid's modulatory potential of PBP3 over ellagic acid. *In silico* evaluations supported the *in vitro* findings as chlorogenic acid exhibited significant antibacterial activity against *P. aeruginosa*, especially in combination with the standard. Hence, chlorogenic acid is a promising lead for development as a PBP3-modulating therapeutic agent. However, added morphology and microscopy-based studies could shed more light on chlorogenic acid's therapeutic effect when used alone or in combination with other antibiotics/compounds, and its precise mechanism of antimicrobial action. This could aid in the development of a broad-spectrum treatment to fight infections caused by clinically relevant microbial strains. Likewise, the structure of chlorogenic acid could be subjected to modification reactions to improve its *in vitro* and *in vivo* antibacterial activities.

Acknowledgments

The authors acknowledge the National Research Foundation (NRF), the Directorate of Research and Postgraduate Support, Durban University of Technology for financial supports, and the Centre for High–Performance Computing (CHPC), South Africa for granting access to the computing systems used in this study.

Disclosure statement

No potential conflict of interest was reported by the author(s).

Funding

This work was supported in part by the Directorate of Research and Postgraduate Support, Durban University of Technology, the South African Medical Research Council (SAMRC) under a Self-Initiated Research Grant and the South African National Research Foundation (NRF) Competitive Programme for Rated Researchers Support [SRUG2204193723] to S. Sabiu.

CreDit authorship contribution statement

Dweba Yamkela: Writing – original draft, Data collection, Investigation. Christiana E. Aruwa: Writing – review & editing. Taofeeq Garuba: Writing – review & editing. Sabiu Saheed: Supervision, Conceptualization, Funding acquisition, Writing – review & editing.

Availability of supporting data

The authors confirm that the data supporting the findings of this study are available within the article and its supplementary materials.

References

[1] Silby MW, Winstanley C, Godfrey SA, et al. Pseudomonas genomes: diverse and adaptable. FEMS Microbiol Rev. 2011;35(4):652–680. doi: 10.1111/j.1574-6976.2011.00269.x

[2] Chapman TM, Perry CM. Cefepime: a review of its use in the management of hospitalised patients with pneumonia. Am J Respir Med. 2003;2(1):75–107. doi: 10.1007/BF03256641

[3] Hancock RE, Speert DP. Antibiotic resistance in *Pseudomonas aeruginosa*: mechanisms and impact on treatment. Drug Resist Updates. 2000;3(4):247–255. doi: 10.1054/drup.2000.0152

[4] Tacconelli E, Akova M, Friedrich AW. Escmid-an international Europe-based society committed to fostering cross-border collaboration and education to improve patient care. Clin Microbiol Infect. 2017;24(1):1–7. doi: 10.1016/j.cmi.2017.05.024 *Policy Commons*.

[5] Hirsch EB, Tam VH. Impact of multidrug-resistant *Pseudomonas aeruginosa* infection on patient outcomes. Expert Rev Pharmacoeconomics & Outcomes Res. 2010;10(4):441–451. doi: 10.1586/erp.10.49

[6] Eckburg PB, Lister T, Walpole S, et al. Safety, tolerability, pharmacokinetics, and drug interaction potential of SPR741, an intravenous potentiator, after single and multiple ascending doses and when combined with β-lactam antibiotics in healthy subjects. Antimicrob Agents Chemother. 2019;63(9):10–11287. doi: 10.1128/AAC.00892-19

[7] Josephine HR, Charlier P, Davies C, et al. Reactivity of penicillin-binding proteins with peptidoglycan-mimetic β-lactams: what's wrong with these enzymes? ACS Chem Biol. 2006;45(51):15873–15883. doi: 10.1021/bi061804f

[8] Sauvage E, Kerff F, Terrak M, et al. The penicillin-binding proteins: structure and role in peptidoglycan biosynthesis. FEMS Microbiol Rev. 2008;32(2):234–258. doi: 10.1111/j.1574-6976.2008.00105.x

[9] Anderson EM, Shaji Saji N, Anderson AC, et al. *Pseudomonas aeruginosa* alters peptidoglycan composition under nutrient conditions resembling cystic fibrosis lung infections. mSystems. 2022;7(3):e00156–22. doi: 10.1128/msystems.00156-22

[10] Verma AK, Ahmed SF, Hossain S, et al. Molecular docking and simulation studies of flavonoid compounds against PBP-2a of methicillin-resistant staphylococcus aureus. J Biomol Struct And Dyn. 2021;3(21):10561–10577. doi: 10.1080/07391102.2021.1944911

[11] Chen W, Zhang YM, Davies C. Penicillin-binding protein 3 is essential for growth of *Pseudomonas aeruginosa*. Antimicrob Agents Chemother. 2017;61(1):10–128. doi: 10.1128/AAC.01651-16

[12] Sahare P, Moon A. *In silico* docking studies of phytoligands against *Escherichia coli* PBP3: approach towards novel antibacterial therapeutic agent. Int J Pharm Sci And Res. 2016;7:3703–3711.

[13] Cobo F. Imported infectious diseases: impact in developed diseases. Woodhead publishing. Communication. 2014;13:122–129.

[14] Abushaheen MA, Fatani AJ, Mansy M, et al. Antimicrobial resistance, mechanisms, and its clinical significance. Disease-A-Month. 2020;66(6):100971. doi: 10.1016/j.disamonth.2020.100971

[15] Freire-Moran L, Aronsson B, Manz C, et al. Critical shortage of new antibiotics in development against multidrug-resistant bacteria—time to react is now. Drug Resist Updates. 2011;14(2):118–124. doi: 10.1016/j.drup.2011.02.003

[16] Adelfo-Escalante A, Carmona SB, Diaz-Quiroz DC, et al. Current perspectives on applications of shikimic and aminoshikimic acids in pharmaceutical chemistry. Res And Rep In Med Chem. 2014;8:35–46. doi: 10.2147/RRMC.S46560

[17] Beutler JA. Natural products as a foundation for drug discovery. Curr Protoc Pharmacol. 2009;46(1):9–11. doi: 10.1002/0471141755.ph0911s46

[18] Bursal E, Köksal E, Gülçin İ, et al. Antioxidant activity and polyphenol content of cherry stem (cerasus avium L.) determined by LC–MS/MS. Food Res Int. 2013;51(1):66–74. doi: 10.1016/j.foodres.2012.11.022

[19] Demir Y, Işık M, Gülçin İ, et al. Phenolic compounds inhibit the aldose reductase enzyme from the sheep kidney. J Biochem Mol Toxicol. 2017;31(9):e21936. doi: 10.1002/jbt.21935

[20] Tzin V, Galili G. New insights into the shikimate and aromatic amino acids biosynthesis pathways in plants. Mol Plant. 2010;3(6):956–972. doi: 10.1093/mp/ssq048

[21] Parthasarathy A, Borrego EJ, Savka MA, et al. Amino acid-derived defence metabolites from plants: a potential source to facilitate novel

antimicrobial development. J Biol Chem. 2021;296:100438. doi: 10.1016/j.jbc.2021.100438

[22] Kroemer RT. Structure-based drug design: docking and scoring. Curr Protein And Peptide Sci. 2007;8(4):312–328. doi: 10.2174/138920307781369382

[23] Durrant JD, McCammon JA. Molecular dynamics simulations and drug discovery. BMC Biol. 2011;9(1):1–9. doi: 10.1186/1741-7007-9-71

[24] Hollingsworth SA, Dror RO. Molecular dynamics simulation for all. Neuron. 2018;99(6):1129–1143. doi: 10.1016/j.neuron.2018.08.011

[25] Hospital A, Goñi JR, Orozco M, et al. Molecular dynamics simulations: advances and applications. Adv And Appl In Bioinf And Chem. 2015:37–47. doi: 10.2147/AABC.S70333

[26] Khan F, Kumar Yadav D, Maurya A, et al. Modern methods & web resources in drug design & discovery. Lett In Drug Des & Discov. 2011;8(5):469–490. doi: 10.2174/157018011795514249

[27] Gandhi RN, Moll A, Sturm WA, et al. Extensively drug-resistant tuberculosis as a cause of death in patients co-infected with tuberculosis and HIV in a rural area in South Africa. Lancet. 2006;368(9547):1575–1580. doi: 10.1016/S0140-6736(06)69573-1

[28] Yoshida H, Kawai F, Obayashi E, et al. Crystal structures of penicillin-binding protein 3 (PBP3) from methicillin-resistant *staphylococcus aureus* in the apo and cefotaxime-bound forms. J Mol Biol. 2012;423(3):351–364. doi: 10.1016/j.jmb.2012.07.012

[29] Aribisala JO, Nkosi S, Idowu K, Astaxanthin-mediated bacterial lethality: evidence from oxidative stress contribution and molecular dynamics simulation. Oxid Med Cell Longev. 2021;2(1):7159652.

[30] Sabiu S, Balogun FO, Amoo SO. Phenolics profiling of *carpobrotus edulis* (l.) N.E.br. And insights into molecular dynamics of their significance in type 2 diabetes therapy and its retinopathy complication. Molecules. 2021;26(16):4867. doi: 10.3390/molecules26164867

[31] Kruse H, Goerigk L, Grimme S. Why the standard b3lyp/6-31g* model chemistry should not be used in dft calculations of molecular thermochemistry: understanding and correcting the problem. J Org Chem. 2012;77(23):10824–10834. doi: 10.1021/jo302156p

[32] Luo J, Xue ZQ, Liu WM, et al. Koopmans' theorem for large molecular systems within density functional theory. J Phys Chem A. 2006;110(43):12005–12009. doi: 10.1021/jp063669m

[33] Calais JL. Density functional theory of atoms and molecules. In: Parr RG, Yang W, editors, International journal of quantum chemistry. Vol. 47. New York, Oxford, 1989. 1989. RG Parr and W Yang, Oxford University Press; 1993. p. 101.

[34] Daina A, Michielin O, Zoete V. SwissADME: a free web tool to evaluate pharmacokinetics, drug-likeness, and medicinal chemistry friendliness of small molecules. Sci Rep. 2017;7(1):42717. doi: 10.1038/srep42717

[35] Banerjee P, Eckert OA, Schrey KA, et al. Protox-ii: a webserver for the prediction of toxicity of chemicals. Nucleic Acids Res. 2018;46(W1):W257–W263. doi: 10.1093/nar/gky318

[36] Balouiri M, Sadiki M, Ibnsouda SK. Methods for in vitro evaluating antimicrobial activity: a review. J Pharm. Anal. 2015;6:71–79.

[37] Basri DF, Xian LW, Abdul Shukor NI, et al. Bacteriostatic antimicrobial combination: antagonistic interaction between epsilon-viniferin and vancomycin against methicillin-resistant *staphylococcus aureus*. Biomed Res Int. 2014;2014:461756. doi: 10.1155/2014/461756

[38] Fahad M, Al-Khodairy M, Kalim A, et al. In silico prediction of mechanism of erysolin-induced apoptosis in human breast cancer cell lines. American. J Bioinf. 2013;9:62–71.

[39] Kufareva I, Abagyan R. Methods of protein structure comparison. Methods In Mol Biol. 2012;957:231–257.

[40] Alhadrami HA, Hamed AA, Hassan HM, et al. Flavonoids as potential anti-mrsa agents through modulation of PBP2a: a computational and experimental study. Antibiotics. 2020;9(9):562. doi: 10.3390/antibiotics9090562

[41] Shode FO, Idowu ASK, Uhomoibhi OJ, et al. Repurposing drugs and identification of inhibitors of integral proteins (spike protein and main protease) of SARS-CoV-2. J Biomol Struct And Dyn. 2021;40(14):6587–6602. doi: 10.1080/07391102.2021.1886993

[42] Rahman A, Deshpande P, Radue MS, et al. A machine learning framework for predicting the shear strength of carbon nanotube-polymer interfaces based on molecular dynamics simulation data. Compos Sci Technol. 2020;207:108627. doi: 10.1016/j.compscitech.2020.108627

[43] Alonso H, Bliznyuk AA, Gready JE. Combining docking and molecular dynamic simulations in drug design. Med Res Rev. 2006;26(5):531–568. doi: 10.1002/med.20067

[44] Mousavi SS, Karami A, Haghighi TM, et al. *In silico* evaluation of Iranian medicinal plant phytoconstituents as inhibitors against main protease and the receptor-binding domain of SARS-CoV-2. Molecules. 2021;26(18):5724. doi: 10.3390/molecules26185724

[45] Ramírez D, Caballero J. Is it reliable to take the molecular docking top scoring position as the best solution without considering available structural data?. Molecules. 2018;23:1038.

[46] Islam R, Parves MR, Paul AS, et al. A molecular modelling approach to identify effective antiviral phytochemicals against the main protease of sars-cov-2. J Biomol Struct Dyn. 2020;39:3213–3224. doi: 10.1080/07391102.2020.1761883

[47] Gajula M, Kumar A, Ijaq J. Protocol for molecular dynamics simulations of proteins. Bio-Protocol. 2016;85(1):159–166. doi: 10.1016/S0006-3495(03)74462-2

[48] Chen D, Oezguen N, Urvil P, et al. Regulation of protein-ligand binding affinity by hydrogen bond pairing. Sci Adv. 2016;2(3):e1501240. doi: 10.1126/sciadv.1501240

[49] Kumar A, Mishra CD, Angadi BU, et al. Inhibition potencies of phytochemicals derived from sesame against SARS-CoV-2 main protease: a molecular docking and simulation study. Front Chem. 2021;9:744376. doi: 10.3389/fchem.2021.744376

[50] Tallei TE, Fatimawali Y, Idroes A, et al. An analysis based on molecular docking and molecular dynamics simulation study of bromelain as anti-SARS-CoV-2 variants. Front Pharmacol. 2021;12:2192. doi: 10.3389/fphar.2021.717757

[51] Huang H, Gong XA. A review of protein inter-residue distance prediction. Curr Bioinf. 2020;15(8):821–830. doi: 10.2174/1574893615999200425230056

[52] Mhatre S, Naik S, Patravale VA. Molecular docking study of EGCG and theaflavin digallate with the druggable targets of SARS-CoV-2. Comput In Biol And Med. 2021;129:104137. doi: 10.1016/j.compbiomed.2020.104137

[53] Aihara JI. Reduced HOMO– LUMO gap as an index of kinetic stability for polycyclic aromatic hydrocarbons. J Phys Chem A. 1999;103(37):7487–7495. doi: 10.1021/jp990092i

[54] Ayers PW, Parr RG, Pearson RG. Elucidating the hard/soft acid/base principle: a perspective based on half-reactions. J Chem Phys. 2006;124(19):1941071–1941078. doi: 10.1063/1.2196882

[55] Olukunle FO, Olowosoke BS, Khalid A, et al. Identification of a 1,8-naphthyridine-containing compound endowed with the inhibition of p53-MDM2/X interaction signalling: a computational perspective. Mol Divers. 2023;28(3):1–19. doi: 10.1007/s11030-023-10637-3

[56] Sylaja B, Gunasekaran S, Srinivasan S. The spectroscopic investigation, NLO, NBO, NMR, HOMO–LUMO and molecular docking analysis on clonazepam. Mater Res Innovations. 2017;22(4):361–373. doi: 10.1080/14328917.2016.1278320

[57] Ma Y, Tao Y, Qu H, et al. Exploration of plant-derived natural polyphenols toward COVID-19 main protease inhibitors: DFT, molecular docking approach, and molecular dynamics simulations. RSC Adv. 2022;12(9):5357–5368. doi: 10.1039/D1RA07364H

[58] Parr RG, Pearson RG. Absolute hardness: companion parameter to absolute electronegativity. J Am Chem Soc. 1983;105(26):7512–7516. doi: 10.1021/ja00364a005

[59] Lipinski CA, Lombardo F, Dominy BW, et al. Experimental and computational approaches to estimate solubility and permeability in drug discovery and development settings. Adv Drug Deliv Rev. 2012;64:4–17. doi: 10.1016/j.addr.2012.09.019

[60] Yamashita F, Hashida M. *In silico* approaches for predicting ADME properties of drugs. Drug Metab Pharmacokinet. 2004;19(5):327–338. doi: 10.2133/dmpk.19.327

[61] Remko M, Bohac A, Kovacikovam L. Molecular structure, PKA, lipophilicity, solubility, absorption, polar surface area, and blood-brain barrier penetration of some antiangiogenic agents. Struct Chem. 2011;22(3):635–648. doi: 10.1007/s11224-011-9741-z

[62] Stephens C, Lucena MI, Andrade RJ. Idiosyncratic drug-induced liver injury: mechanisms and susceptibility factors. Compr Toxicol. 2018;2:625–650.

[63] Gao Y, Gesenberg C, Zheng W. Oral formulations for preclinical studies: principle, design, and development considerations. Dev Solid Oral Dosage Forms Academic Press. 2017;2:455–495.

[64] Vinarov Z, Abdallah M, Agundez JAG, et al. Impact of gastrointestinal tract variability on oral drug absorption and pharmacokinetics: an UNGAP review. Eur J Pharm Sci. 2021;162:105812. doi: 10.1016/j.ejps.2021.105812

[65] Parsons RL. Drug absorption in gastrointestinal disease with particular reference to malabsorption syndromes. Clin Pharmacokinet. 1977;2(1):45–60. doi: 10.2165/00003088-197702010-00004

[66] Fasinu P, Pillay V, Ndesendo VM, et al. Diverse approaches for the enhancement of oral drug bioavailability. Biopharmaceutics And Drug Dispos. 2011;32(4):185–209. doi: 10.1002/bdd.750

[67] Daneman R, Prat A. The blood–brain barrier. Cold Spring Harb Perspect Biol. 2015;7(1): a020412. doi: 10.1101/cshperspect.a020412

[68] Michely JA, Meyer MR, Maurer HH. Power of Orbitrap-based lc-high resolution-ms/ms for comprehensive drug testing in urine with or without conjugate cleavage or using dried urine spots after on-spot cleavage in comparison to established LC–MS n or GC–MS procedures. Drug Test Anal. 2018;10(1):158–163. doi: 10.1002/dta.2255

[69] Parasuraman S. Toxicological screening. J Pharmacol And Pharmacother. 2011;2 (2):74–79. doi: 10.4103/0976-500X.81895

[70] Schulz M, Iwersen-Bergmann S, Andresen H, et al. Therapeutic and toxic blood concentrations of nearly 1,000 drugs and other xenobiotics. Crit Care. 2012;16(4):1–4. doi: 10.1186/cc11441

[71] Gulati K, Ray A. Immunotoxicity. Handb Of Toxicol Of Chem Warfare Agents, Academic Press 2009;40:595–609.

[72] Hentz KL. Safety assessment of pharmaceuticals. In: comprehensive toxicology 2nd ed. Elsevier. 2010;3:17–28.

[73] Bailey K. Physiological factors affecting drug toxicity. Regul Toxicol Pharmacol. 1983;3 (4):389–398. doi: 10.1016/0273-2300(83)90009-0

[74] Saibabu V, Fatima Z, Khan LA, et al. Therapeutic potential of dietary phenolic acids. Adv Pharmacol Sci. 2015;2015:823539. doi: 10.1155/2015/823539

[75] Lou Z, Wang H, Zhu S, et al. Antibacterial activity and mechanism of action of chlorogenic acid. J Food Sci. 2011;76(6):M398–M403. doi: 10.1111/j.1750-3841.2011.02213.x

[76] Moellering RC Jr. Rationale for use of antimicrobial combinations. Am J Med. 1983;75 (2):4–8. doi: 10.1016/0002-9343(83)90088-8

[77] Bellio P, Fagnani L, Nazzicone L, et al. New and simplified method for drug combination studies by checkerboard assay. MethodsX. 2021;8:101543. doi: 10.1016/j.mex.2021.101543

[78] Qin R, Xiao K, Li B, et al. The combination of catechin and epicatechin gallate from fructus crataegi potentiates β-lactam antibiotics against methicillin-resistant staphylococcus aureus (MRSA) in vitro and in vivo. Int J Mol Sci. 2013;14(1):1802–1821. doi: 10.3390/ijms14011802

[79] Bassole IH, Juliani HR. Essential oils in combination and their antimicrobial properties. Molecules. 2012;17(4):3989–4006. doi: 10.3390/molecules17043989

[80] Cascorbi I. Drug interactions—principles, examples, and clinical consequences. Dtsch Arztebl Int. 2012;109:546. doi: 10.3238/arztebl.2012.0546

[81] Aiyegoro OA, Afolayan AJ, Okoh AI. In vitro antibacterial time-kill studies of leaves extracts of *helichrysum longifolium*. J Med Plants Res. 2009;3:462–467.

[82] Grégoire N, Raherison S, Grignon C, et al. Semimechanistic pharmacokinetic-pharmacodynamic model with adaptation development for time-kill experiments of ciprofloxacin against Pseudomonas aeruginosa. Antimicrob Agents Chemother. 2010;54:2379–2384.